Published OnlineFirst December 10, 2012; DOI: 10.1158/1078-0432.CCR-12-2692

Clinical Cancer Research

Antitumor Activity of Cell-Permeable RUNX3 Protein in Gastric Cancer Cells

Junghee Lim, Tam Duong, Nga Do, et al.

Clin Cancer Res 2013;19:680-690. Published OnlineFirst December 10, 2012.

Published OnlineFirst December 10, 2012; DOI: 10.1158/1078-0432.CCR-12-2692

Cancer Therapy: Preclinical

Clinical Cancer Research

Antitumor Activity of Cell-Permeable RUNX3 Protein in Gastric Cancer Cells

Junghee Lim[1,4], Tam Duong[2], Nga Do[2], Phuong Do[2], Jaetaek Kim[3], Hyuncheol Kim[4], Wael El-Rifai[5], H. Earl Ruley[6], and Daewoong Jo[1,2,5]

Abstract

Purpose: Gastric cancer is a leading cause of cancer death worldwide. Limited therapeutic options highlight the need to understand the molecular changes responsible for the disease and to develop therapies based on this understanding. The goal of this study was to develop cell-permeable (CP-) forms of the RUNT-related transcription factor 3, RUNX3–a candidate tumor suppressor implicated in gastric and other epithelial cancers–to study the therapeutic potential of RUNX3 in the treatment of gastric cancer.

Experimental Design: We developed novel macromolecule transduction domains (MTD) which were tested for the ability to promote protein uptake by mammalian cells and tissues and used to deliver of biologically active RUNX3 into human gastric cancer cells. The therapeutic potential CP-RUNX3 was tested in the NCI-N87 human tumor xenograft animal model.

Results: RUNX3 fusion proteins, $HM_{57}R$ and $HM_{85}R$, containing hydrophobic MTDs enter gastric cancer cells and suppress cell phenotypes (e.g., cell-cycle progression, wounded monolayer healing, and survival) and induce changes in biomarker expression (e.g., $p21^{Waf1}$ and VEGF) consistent with previously described effects of RUNX3 on TGF-β signaling. CP-RUNX3 also suppressed the growth of subcutaneous human gastric tumor xenografts. The therapeutic response was comparable with studies augmenting *RUNX3* gene expression in tumor cell lines; however, the protein was most active when administered locally, rather than systemically (i.e., intravenously).

Conclusions: These results provide further evidence that RUNX3 can function as a tumor suppressor and suggest that practical methods to augment RUNX3 function could be useful in treating of some types of gastric cancer. *Clin Cancer Res; 19(3); 680–90. ©2012 AACR.*

Introduction

Gastric cancer is the most common cancer in Asian countries (e.g., Korea and Japan) and a leading cause of cancer death worldwide, provoking considerable effort to understand the pathogenesis of the disease and to develop improved methods for diagnosis and treatment (1, 2). Gastric tumors arise by multiple etiologies, including an intestinal type that emerges through a metaplasia–dysplasia–carcinoma sequence in which inflammatory responses to *Heliobacter pylori* infection play an initiating role and a diffuse type that arise without clearly defined precursor lesions or etiology. Therapeutic options are limited for gastric cancers not cured by surgical resection, and overall 5-year survival rates are in the range of 30% (1). As a consequence, there is considerable interest in characterizing the molecular changes responsible for tumor type and grade to better predict disease outcome and possibly to inform individualized therapies (2).

RUNT-related transcription factor 3 (RUNX3) has been implicated as a tumor suppressor gene in gastric cancers (3) as well as a variety of malignancies (4). *Runx3* knockout mice develop gastric hyperplasia and tumors, associated with reduced levels of apoptosis, altered cellular responses to TGF-β (5) and changes in the cyclin-dependent kinase inhibitor $p21^{Waf1}$ and VEGF expression consistent with enhanced proliferation and angiogenesis, respectively (6, 7). Reductions in RUNX3 expression have been attributed to promoter hypermethylation (8), LOH, and protein mislocalization (9) and correlate with poor prognosis (10–13). Conversely, enforced *RUNX3* expression suppresses the proliferation and tumorigenicity of gastric cancer cell lines (3, 7, 10).

However, other studies have challenged the concept that RUNX3 functions directly as a tumor suppressor in gastric

Authors' Affiliations: [1]ProCell R&D Institute, ProCell Therapeutics, Inc., Seoul; [2]Department of Biomedical Sciences, Chonnam National University Medical School, Kwangju; [3]Department of Internal Medicine, College of Medicine, Chung-Ang University, Seoul; [4]Interdisciplinary Program of Integrated Biotechnology, Sogang University, Seoul, Korea; and [5]Departments of Surgery and Cancer Biology; [6]Department of Pathology, Microbiology & Immunology, Vanderbilt University School of Medicine, Nashville, Tennessee

Note: Supplementary data for this article are available at Clinical Cancer Research Online (http://clincancerres.aacrjournals.org/).

Corresponding Author: Daewoong Jo, Department of Surgery, Vanderbilt University School of Medicine, 1255 MRB IV, 2215B Garland Avenue, Nashville, TN 37232. Phone: 615-322-8207; Fax: 615-322-7852; E-mail: dae-woong.jo@vanderbilt.edu

doi: 10.1158/1078-0432.CCR-12-2692

Published OnlineFirst December 10, 2012; DOI: 10.1158/1078-0432.CCR-12-2692

Translational Relevance

Advances in understanding the molecular changes responsible for gastric cancer etiology and progression are expected to improve disease diagnosis and treatment. RUNX3 has been implicated as a tumor suppressor gene in gastric cancers; however, this claim is controversial. Using macromolecule intracellular transduction technology, we developed the first cell-permeable (CP-) RUNX3 protein which suppressed cell phenotypes and induced changes in biomarker expression consistent with previously described effects of RUNX3 on TGF-β signaling. The protein also suppressed the growth of human gastric tumors in a mouse xenograft model. These results are consistent with the idea that RUNX3 can function as a tumor suppressor in gastric cancer. Gastric cancer is a leading cause of cancer death; however, only limited therapeutic options are available for tumors not cured by surgical resection. The present study illustrates the use of protein-based therapies to target gastric cancer.

cancer (14–17). The murine gene does not appear to be expressed in epithelial cells of the developing or adult gastrointestinal tract (16) and therefore cannot exert cell-intrinsic tumor-suppressing effects under normal, steady-state conditions. The gastric hyperplasia observed in *Runx3* knockout mice may be a secondary consequence of autoimmune colitis (14), a common consequence of impaired TGF-β signaling in T lymphocytes (18–20). It remains to be determined whether RUNX3 is expressed in normal human gut epithelium, although the absence of such expression does not preclude a tumor-suppressive role, assuming RUNX3 is induced in response to malignant change. This could also account for low levels of RUNX3 expression observed in some gastric cancer cell lines.

In the present report, we investigated the use of macromolecule intracellular transduction technology (MITT) to deliver biologically active RUNX3 protein into gastric cancer cells, grown both in culture and as tumor xenografts. MITT was used previously to deliver peptides and proteins to a variety of tissues (notably liver, lung, pancreas, and lymphoid tissues), resulting in dramatic protection against lethal inflammatory diseases (21–25), suppression of pulmonary metastases (26), and inhibition of subcutaneous tumor xenografts (27). The technology exploits the ability of hydrophobic macromolecule transduction domains (MTD) to promote bidirectional transfer of peptides and proteins across the plasma membrane (27–29). In contrast, cationic protein transduction domains (PTD; e.g., those derived from HIV Tat and Antennapedia) enhance protein uptake predominately through absorptive endocytosis and macropinocytosis, which sequester significant amounts of protein into membrane-bound and endosomal compartments and limit cell-to-cell spread within tissues (30, 31). However, cellular uptake and systemic delivery are both heavily influenced by the cargo, such that the use of any protein transduction approach must be investigated on a case-by-case basis (30–32). In the present study, we developed a cell-permeable RUNX3 protein to examine the direct effects of RUNX3 in living cells under non–steady-state conditions and to investigate the feasibility of using RUNX3 as a protein-based therapy for gastric cancer.

Materials and Methods

Expression and purification of MTD fusion proteins

MTD13, MTD57, and MTD108 were derived from signal sequences from NP_639877, CAD0547.1, NP_629842.1, and NP_003842, respectively, as previously described (26, 27). Histidine-tagged fusion proteins containing EGFP or the full-length 46-kDa RUNX3 protein (33) and MTD13, MTD57, MTD85, MTD108, the FGF4 MTS (M_m, AAVLLPVLLAAP), or a random sequence (S, SANVEPLERL) were cloned into pET-28a(+) (Novagen) and expressed in *Escherichia coli* BL21-CodonPlus (DE3) cells.

Histidine-tagged recombinant proteins were purified on a Qiagen Ni^{2+} affinity resin under denaturing conditions and refolded by dialysis against 0.55 mol/L guanidine HCl, 0.44 mol/L L-arginine, 50 mmol/L Tris-HCl, 150 mmol/L NaCl, 1 mmol/L EDTA, 100 mmol/L NDSB, 2 mmol/L reduced glutathione, and 0.2 mmol/L oxidized glutathione for 48 hours at 4°C and then changed to RPMI-1640 medium. Proteins were quantified by the Bradford method (Bio-Rad), were aliquoted, and stored at −20°C. The purified proteins were judged to have minimum levels of endotoxin as assessed by the limulus amebocyte lysate (LAL) assay (Associates of Cape Cod, Inc.). Recombinant proteins were named using the following convention: H, R, and M stand for the His tag, RUNX3, and MTD, respectively. Histidine-tagged recombinant proteins were HR (His-RUNX3), HM_m R (His-MTS-RUNX3), HRM_m (His-RUNX3-MTS), HM_m RM_m (His-MTS-RUNX3-MTS), $HM_{57}R$ (His-MTD57-RUNX3), and $HM_{85}R$ (His-MTD85-RUNX3).

Protein uptake and tissue distribution

Recombinant proteins were conjugated to 5/6-FITC and uptake by cultured RAW 264.7 and NIH3T3 cells were assessed as described previously (26, 27). Briefly, the cells were treated with 10 μmol/L fluorescein isothiocyanate (FITC)-labeled proteins for 1 hour at 37°C, washed with cold PBS three times, and treated with proteinase K (10 μg/mL) for 20 minutes at 37°C to remove cell surface–bound proteins. Protein uptake was quantified by flow cytometry (FACSCalibur; BD Biosciences). Balb/c mice (6-week-old, female) were injected intraperitoneally (300 μg/head) with FITC only or FITC-conjugated proteins. After 2 hours, the liver, kidney, spleen, lung, heart, and brain were isolated, washed with an O.C.T. compound (Sakura), and frozen on dry ice. Cryosections (15 μm) were analyzed by fluorescence microscopy.

Western blot analysis

Human gastric cancer cell lines MKN28 and NCI-N87 (Korean Cell Line Bank, Seoul, Korea) were cultured in

Published OnlineFirst December 10, 2012; DOI: 10.1158/1078-0432.CCR-12-2692

RPMI-1640 medium and maintained at 37°C in an atmosphere containing 5% CO_2. A total of 5×10^6 cells (plated the previous day) were incubated with or without 2 ng/mL TGF-β for 24 hours and then treated with 10 μmol/L of RUNX3 proteins (HR, HM_mR, HRM_m, HM_mRM_m, $HM_{57}R$, and $HM_{85}R$) for 1 hour. Cells were lysed either immediately (Rb phosphorylation) or after 12 hours [$p21^{Waf1}$, $p27^{Kip1}$, proliferating cell nuclear antigen (PCNA), cleaved caspase-3, cyclin A, cyclin E, and VEGF expression] in 200 μL ice-cold lysis buffer (20 mmol/L HEPES, pH 7.2, 1% Triton-X, 10% glycerol) and centrifuged at 12,000 rpm for 20 minutes at 4°C. Supernatants were assayed for protein content (Bio-Rad Bradford Protein Assay) and stored at −80°C until use. The antibodies for $p21^{Waf1}$ and cleaved caspase-3 were from Cell Signaling Technology, and the antibodies for $p27^{Kip1}$, PCNA, cyclin A, cyclin E, phospho-Rb (Ser807/811), and VEGF were from Santa Cruz Biotechnology. The secondary antibody was goat anti-mouse IgG-HRP (Santa Cruz Biotechnology).

Wound-healing assay

MKN28 and NCI-N87 cells were incubated with TGF-β (2 ng/mL) for 24 hours and washed extensively with PBS. The cells were then treated with 10 μmol/L HR, HM_mRM_m, $HM_{57}R$, or $HM_{85}R$ for 1 hour in serum-free medium. The cells were washed twice with PBS, and the monolayer at the center of the well was "wounded" by scraping with a pipette tip. Cell proliferation and/or migration were observed by phase contrast microscopy.

Effects of CP-RUNX3 on cell proliferation and survival

NCI-N87 cells were treated with 5 μmol/L HR, HM_mRM_m, $HM_{57}R$, or $HM_{85}R$ for 1 hour at 37°C and analyzed for changes in DNA content and cell survival. To monitor changes in DNA content, the cells were washed twice with cold PBS, resuspended in 200 μL cold PBS, and fixed by gradual addition of 4-mL cold 70% ethanol, washed twice with cold PBS, and re-suspended in PI master mix [40 μg/mL propidium iodide (PI), 100 μg/mL DNase-free RNase in PBS] at a final cell density of 0.5×10^6 cell/mL. The cell mixtures were incubated at 37°C for 30 minutes before analysis by flow cytometry. Changes in cell viability were determined by using the sulforhodamine B (SRB) assay (34) after treating cells with recombinant proteins for 72 hours. The cells were fixed and stained by the addition of 0.4% (w/v) SRB in 1% acetic acid solution. Loss of cell viability was assessed by increased SRB staining as determined by increased absorbance at 540 nm.

Apoptotic and necrotic cells were analyzed using an Annexin-V assay kit (BD Biosciences). Briefly, treated cells were washed twice with cold PBS and resuspended in binding buffer (10 mmol/L HEPEPS, 140 mmol/L NaCl, 25 mmol/L $CaCl_2$, pH 7.4) at a concentration of 1×10^6 cells/mL. The cells were then treated with a solution containing FITC-labeled Annexin-V and PI solution, followed by analysis on a FACSCalibur (BD Biosciences).

Xenograft tumor model

Five-week-old, immunodeficient Balb/c *nu/nu* mice (Central Lab. Animal Inc.) were subdivided into 4 groups of 5 mice each. NCI-N87 cells were administered to the left upper back of the mouse via subcutaneous injection at a concentration of 1×10^7 cells/mL. Once the tumor size was measured as 60 to 80 mm^3 (width^2 × length × 0.5), the protein (HR, $HM_{57}R$, or $HM_{85}R$) or diluent (PBS) was administered daily for 21 days (100 μg/mouse, 5 mg/kg, 100 μL) via subcutaneous injection at the left upper back of the mouse, at sites adjacent to the tumor. Tumor size was monitored by measuring the longest (length) and shortest dimensions (width) once a day with a dial caliper, and tumor volume was calculated as width^2 × length × 0.5. Alternatively, mice ($n = 10$/group) were treated with proteins via daily intravenous injection in the lateral tail vein for 21 days (300 μg/mouse, 15 mg/kg, 300 μL).

Histological analysis of protein expression and apoptosis

$p21^{Waf1}$ and VEGF expression in tumors was assessed by immunohistochemical staining of paraffin-embedded sections 21 and 35 days after starting protein therapy as described previously (26, 27). Tissue sections were stained with anti-$p21^{Waf1}$ (Cell Signaling Technology) or VEGF (Santa Cruz Biotechnology) primary antibodies and with goat anti-mouse IgG-HRP (Biogenex) secondary antibody and counterstained with hematoxylin. Apoptosis in tumor sections was analyzed 21 days after starting protein therapy by the *In situ* Cell Death Detection Kit, TMR red (Roche), and ApopTag Red *In Situ* Apoptosis Detection Kit (Chemicon, Billerica) as specified by the suppliers. Reverse-transcription PCR (RT-PCR) analysis was conducted using total RNAs isolated from tumor tissues at day 21.

Statistical analysis

All experimental data obtained from cultured cells are expressed as the means ± SD. Statistical significance was evaluated using a one-tailed Student *t* test. For animal testing, paired *t* tests for comparisons between and within groups were used to determine the significance of the differences in tumor volume *in vivo*. Statistical significance was established at $P < 0.05$.

Results

Development of cell-permeable RUNX3 proteins

MTD57 and MTD85 were identified from a screen of 1,500 potential hydrophobic signal peptides for sequences with protein transduction activity as assessed using an EGFP reporter protein. Sequences spanning amino acids 1–23 of CAD0547.1 and 20–42 of NP_629842.1 were subsequently modified to LIALLAAPLA and LLAAAAALLLA, respectively (Supplementary Table S1). Both peptides promoted greater cellular uptake of an EGFP cargo protein by cultured NIH3T3 cells than the reference membrane translocating sequence, MTS (M_m), derived from the hydrophobic signal peptide of fibroblast growth factor 4 (FGF4; Supplementary

Published OnlineFirst December 10, 2012; DOI: 10.1158/1078-0432.CCR-12-2692

Fig. S1A). Their relative cell permeability to the FGF4-MTS was 1.8- and 4.8-fold (Supplementary Fig. S1B). Finally, MTD57, MTD85, and the FGF4 MTS all enhanced the systemic delivery of EGFP proteins to a variety of tissues, including liver, kidney, spleen, lung, heart, and brain after intraperitoneal injection, although the $HM_{85}E$ and HM_mE showed greater tissue distribution 48 hours postinjection than $HM_{57}E$ (Supplementary Fig. S1C). In contrast, HSE, an EGFP protein containing a random sequence (Supplementary Fig. S1C) instead of an MTD, did not accumulate in distal tissues.

RUNX3 fusion proteins containing MTD57, MTD85, and the FGF4 MTS along with a 6× histidine tag and nuclear localization signal (NLS) from SV40 large T antigen (Fig. 1A) were expressed in *E. coli* DE3 cells, purified under denaturing conditions (Fig. 1B) and refolded, with yields of soluble protein ranging from 2 to 36 mg/L (Fig. 1A). The NLS sequence was included first to enhance nuclear localization (based on our experience with other CP proteins) given reports that RUNX3, which is a nuclear transcription factor, may be inactivated by processes in tumor cells that cause the protein to localize to the cytoplasm (9) and second to enhance the solubility of MTD-containing recombinant proteins.

To examine protein uptake, the recombinant proteins were conjugated to 5/6-FITC and incubated with NIH3T3 cells at (10 mmol/L for 1 hour at 37°C). The cells were washed 3 times with ice-cold PBS, treated with proteinase K (10 mg/mL for 20 minutes at 37°C) to remove surface-bound proteins, nuclei were counterstained with 1 mg/mL propidium iodide, and internalized proteins were visualized by confocal laser scanning microscopy (Fig. 2A). RUNX3 proteins containing MTD57 ($HM_{57}R$) or MTD85 ($HM_{85}R$) or the FGF4 MTS (HM_m, HRM_m and HM_mRM_m) efficiently entered cells and were localized to various extents in both the nucleus and cytoplasm. In contrast, a RUNX3 protein (HR) containing only the 6×His and NLS sequences did not appear to enter cells (Fig. 2A). While $HM_{57}R$ and $HM_{85}R$ both entered cells, $HM_{85}R$ displayed more uniform cellular distribution, and the protein was more soluble. As with the EGFP cargo, protein uptake of $HM_{85}R$ by RAW264.7 cells was also very efficient (Fig. 2B). In addition, MTD85 enhanced the systemic delivery of RUNX3 protein to a variety of tissues (liver, kidney, spleen, lung, heart, and,

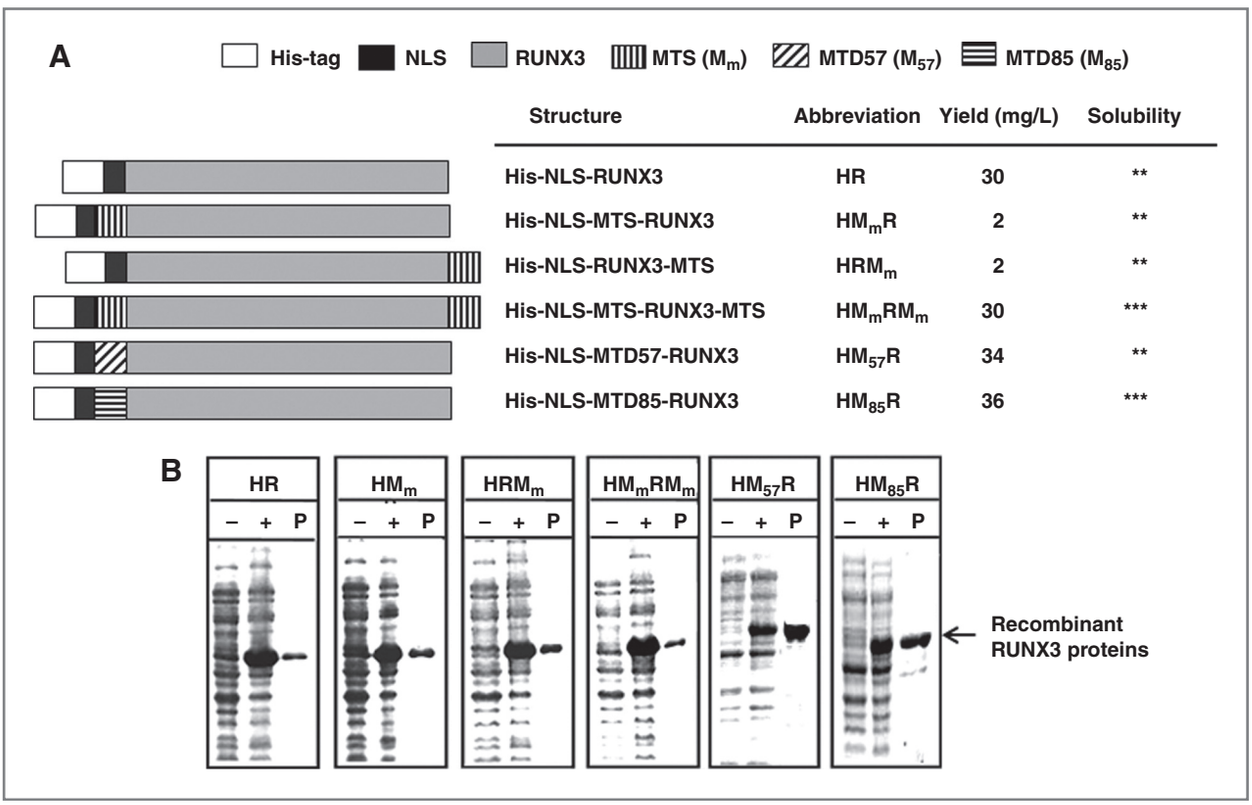

Figure 1. Structure and expression of MTD-RUNX3 fusion proteins. RUNX3 fusion proteins were expressed and purified. A, structure of His-tagged RUNX3 proteins containing MTD57 or MTD85. H, M_m, M_{57}, M_{85}, and R refer to 6× His tag (▭), the FGF4 MTS (▭), MTD57 (▨),MTD85 (▭), and RUNX3 (▭), respectively. An NLS from SV40 T antigen is also shown (■). The size (number of amino acids) and yield (mg/L) of each recombinant protein is indicated. B, protein expression in *E. coli*. SDS-PAGE analysis of cell lysates before (–) and after (+) induction with IPTG and aliquots of Ni^{2+} affinity–purified proteins. The mobility of recombinant RUNX3 proteins is indicated. Solubility was scored on a 4-point scale ranging from highly soluble proteins with little tendency to precipitate (****) to largely insoluble proteins (*).

Published OnlineFirst December 10, 2012; DOI: 10.1158/1078-0432.CCR-12-2692

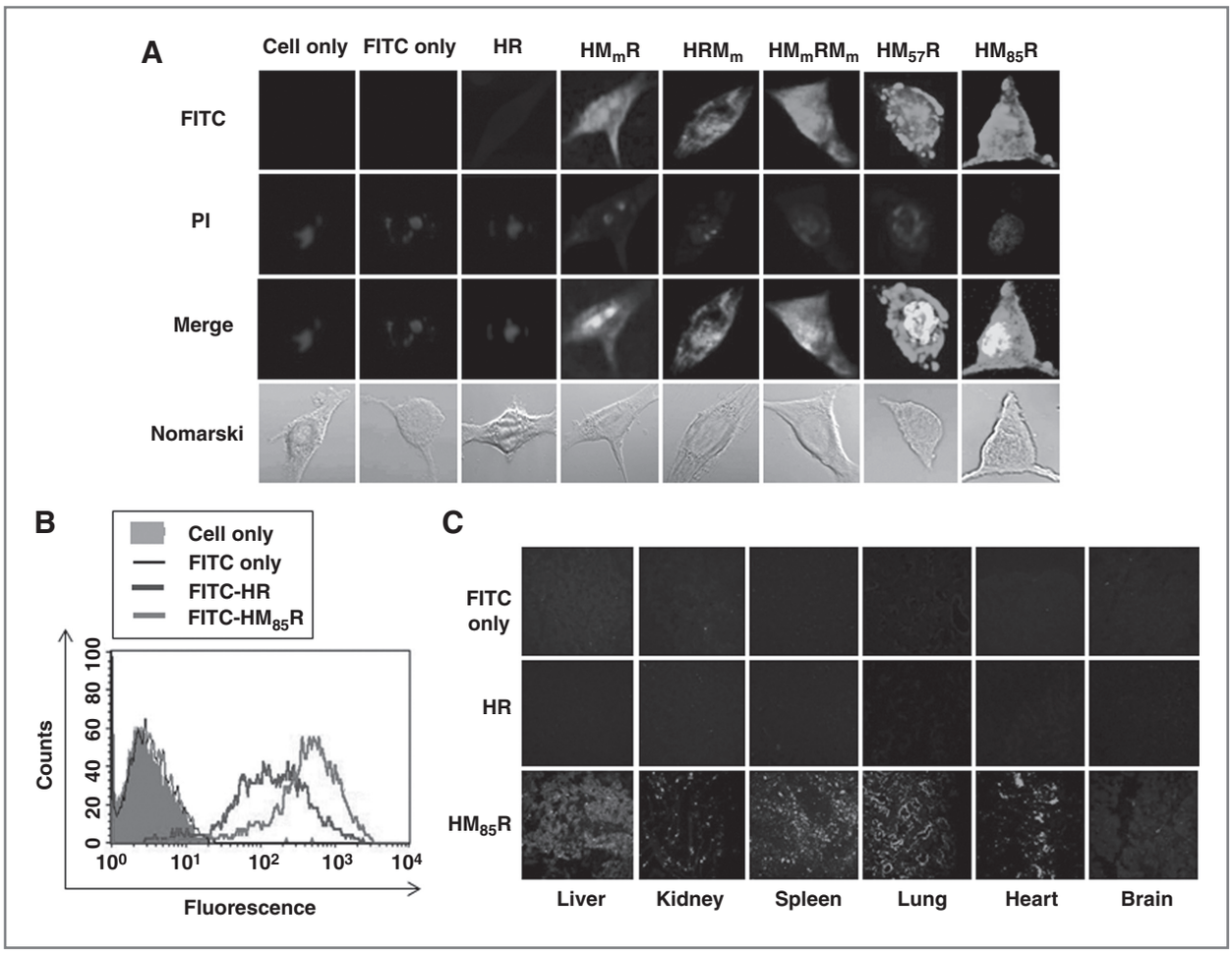

Figure 2. Efficient MTD-mediated RUNX3 protein delivery into cells and tissues. CP-RUNX3 proteins efficiently entered cells and were localized in both the nucleus and cytoplasm. $HM_{85}R$ was systemically delivered to a variety of tissues. A, RUNX3 protein uptake by NIH3T3 cells. NIH3T3 cells were incubated with 10 μmol/L FITC-conjugated recombinant MTD-RUNX3 proteins, an equimolar concentration of unconjugated FITC (FITC only) or vehicle (culture medium RPMI-1640) for 1 hour, washed and treated with proteinase K to remove noninternalized protein, and visualized by fluorescence confocal laser scanning microscopy. B, uptake of MTD-RUNX3 protein ($HM_{85}R$) by RAW264.7 cells. Cells were exposed to 10 μmol/L of the FITC conjugated RUNX3 proteins containing MTD85 ($HM_{85}R$, red) or lacking MTD (HR, blue) or 10 μmol/L of FITC alone (black thin line) for 1 hour, treated to remove cell-associated but noninternalized protein, and analyzed by flow cytometry. C, systemic RUNX3 protein delivery to murine tissues. Cryosections (15 μm) of saline-perfused organs were prepared from mice 2 hours after intraperitoneal injection of 20 μg FITC or 300 μg FITC-labeled RUNX3 proteins with ($HM_{85}R$) and without (HR) the MTD85 sequence. Uptake (A) and tissue distribution (B) of the recombinant proteins (green staining) was assessed by fluorescence microscopy.

to a lesser extent, brain) after intraperitoneal injection (Fig. 2C).

RUNX3 proteins with MTD13 (LAAAALAVLPL) and MTD108 (ALLAALLAP) in place of MTDs 57 and 85 were also evaluated, but the proteins were less soluble, produced lower yields when expressed in *E. coli*, and entered cells less efficiently (data not shown); therefore, these proteins were not evaluated further.

Biological activities of cell-permeable RUNX3

RUNX3 participates in TGF-β signaling by interacting with SMADs to influence the TGF-β regulated gene expression and inhibit cell-cycle progression. We therefore examined the effects of CP-RUNX3 on cell proliferation and associated biomarker expression in human gastric cancer cell lines, NCI-N87 and MKN28. NCI-N87 cells were incubated in normal culture media either lacking or containing TGF-β and treated with the recombinant RUNX3 proteins fused to a reference MTS (HM_mRM_m), an MTD ($HM_{57}R$ and $HM_{85}R$), or a RUNX3 protein lacking an MTD (HR; Fig. 3A). While TGF-β alone produced only modest changes in biomarker expression (cell only in Fig. 3A), the cell-permeable forms of RUNX3 suppressed the cyclin A, cyclin E, and VEGF expression and Rb phosphorylation, as assessed by Western blotting. Changes in biomarker expression were greater in the presence than absence of TGF-β, and the greatest suppression was observed with $HM_{85}R$, followed by $HM_{57}R$, whereas HM_mRM_m produced the smallest effect. Similar results were obtained in the presence of TGF-β using another gastric cancer cell line (MKN28), and the cell-permeable

Published OnlineFirst December 10, 2012; DOI: 10.1158/1078-0432.CCR-12-2692

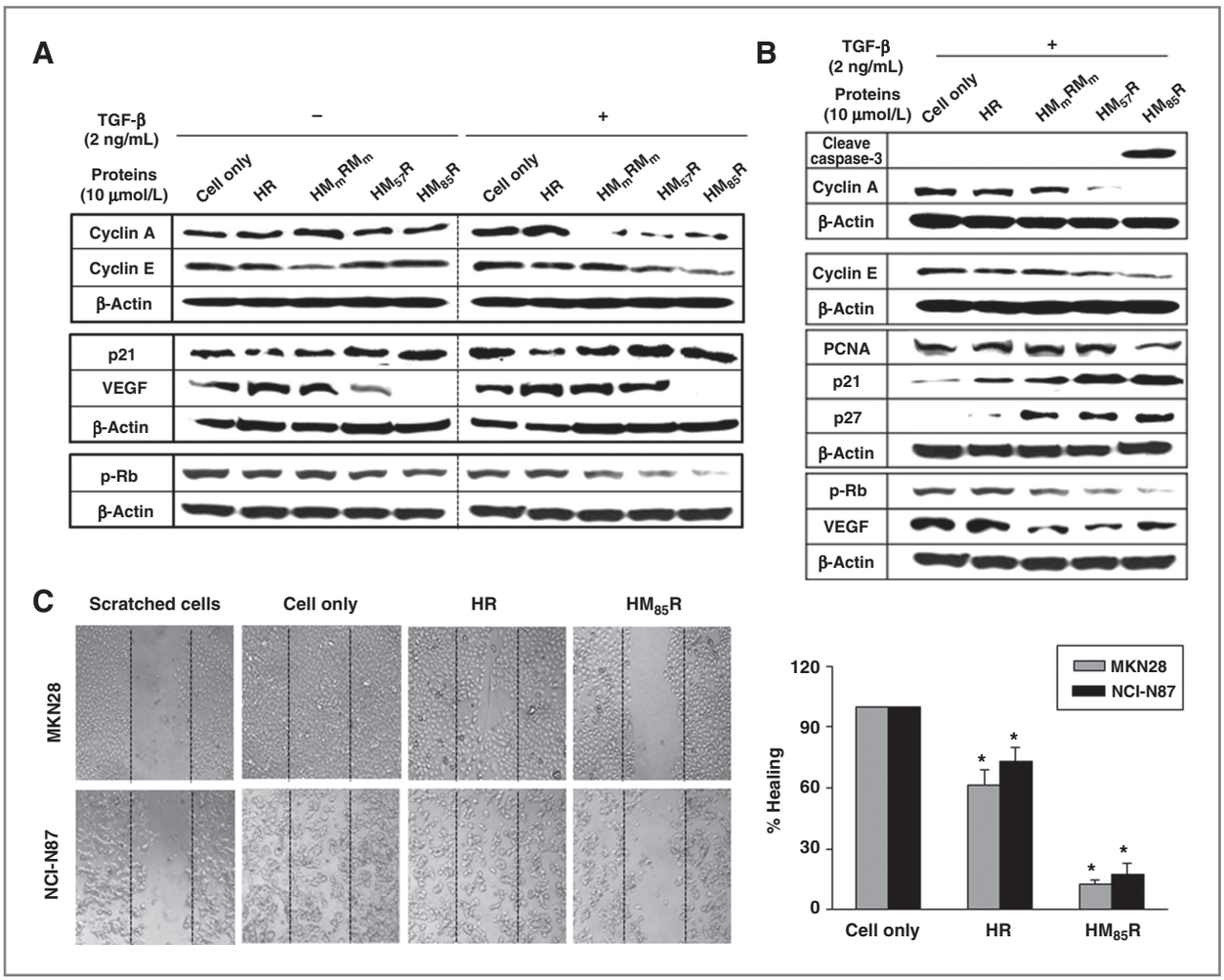

Figure 3. CP-RUNX3 protein induces changes in biomarker expression and suppresses cell phenotypes—cell-cycle re-entry and wound healing—in the presence of TGF-β. CP-RUNX3 suppressed the cyclin A, cyclin E, and VEGF expression and Rb phosphorylation, enhanced the expression of the $p21^{Waf1}$ and $p27^{Kip1}$, suppressed the expression of PCNA, and stimulated caspase-3 cleavage in gastric cancer cells in the presence of TGF-β. CP-RUNX3 proteins also suppressed proliferation of cancer cells. A and B, Western blot analyses. NCI-N87 (A) or MKN28 cells (B) incubated without (–) or with (+) TGF-β (2 ng/mL) for 24 hours and treated for 1 hour with 10 μmol/L recombinant RUNX3 proteins fused to FGF4-derived MTS (HM_mR, HRM_m, or HM_mRM_m), MTD57 ($HM_{57}R$), MTD85 ($HM_{85}R$), or no MTD (HR). Cells were treated with proteins in serum-free media and lysed immediately to analyze Rb phosphorylation or incubated an additional 12 hours in serum-containing media to detect cleaved caspase-3, $p21^{Waf1}$, $p27^{Kip1}$, PCNA, cyclin A, cyclin E, and VEGF. C, Wound-healing assay. Cell monolayers were incubated with TGF-β (2 ng/mL) for 24 hours, treated with HR or $HM_{85}R$ proteins for 1 hour in serum-free media, visualized and (left), and analyzed statistically (right) after an additional 48 hours in normal growth media. Photographed data shown here are representative of 3 independent assays. The data are presented as means ± SD ($n = 3$). *, $P < 0.01$ as determined by a Student unpaired t test.

RUNX3 proteins also enhanced the expression of the cyclin-dependent kinase inhibitors, $p21^{Waf1}$ and $p27^{Kip1}$, and suppressed the expression of PCNA (Fig. 3B). Finally, $HM_{85}R$ stimulated caspase-3 cleavage, a pro-apoptotic marker (Fig. 3B).

We next examined the ability of cell-permeable RUNX3 to influence cell-cycle re-entry, migration, or proliferation as assessed by a monolayer-wounding assay. Gastric cancer cells MKN28 and NCI-N87 pretreated with 2 ng/mL TGF-β were treated with recombinant proteins for 1 hour, the monolayers were wounded, and cell migration/proliferation in the wound was monitored (Fig. 3C, left) and analyzed statistically (Fig. 3C, right) after 48 hours. All CP-RUNX3 proteins tested (HM_mRM_m, $HM_{57}R$, and $HM_{85}R$) suppressed repopulation of the wounded monolayer; however, $HM_{85}R$ produced the greatest inhibitory effect in both cell lines by 88% in MKN28 and 82% in NCI-N87 cells, respectively. In light of these results, $HM_{85}R$ was selected as the most active CP-RUNX3 protein for further evaluation as a potential antitumor agent.

Activation of caspase-3 in $HM_{85}R$-treated cancer cells led us to examine the effects of CP-RUNX3 on apoptosis and necrosis. The effects of treating of NCI-N87 cells with $HM_{85}R$ after 72 hours included substantial loss of cell viability as assessed by the SRB assay (Fig. 4A), enhanced Annexin-V staining (Fig. 4B), and accumulation of cells

Published OnlineFirst December 10, 2012; DOI: 10.1158/1078-0432.CCR-12-2692

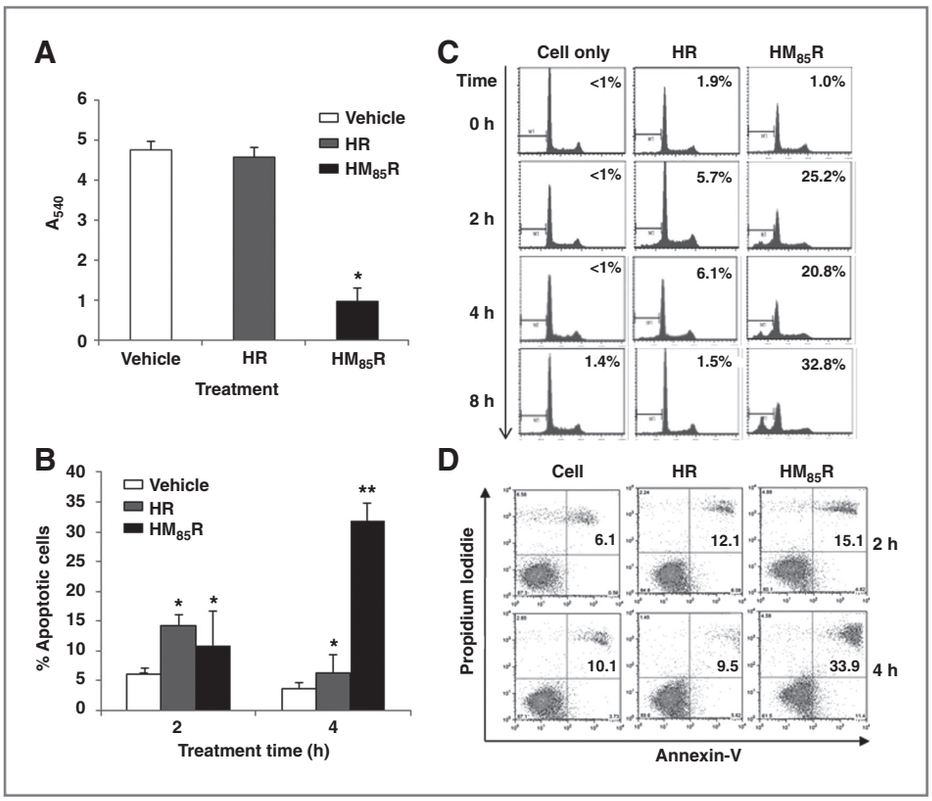

Figure 4. Cell-permeable RUNX3 induces apoptosis/necrosis. $HM_{85}R$ treatment induced substantial loss of cell viability induced by apoptosis/necrosis in the gastric cancer cells. A, SRB-binding assay. NCI-N87 cells were treated for 1 hour with 10 μmol/L HR or $HM_{85}R$ proteins, and cell viability was assessed 72 hours later by the SRB-binding assay. Loss of cell viability induced by CP-RUNX3 ($HM_{85}R$) and not control RUNX3 protein without the MTD sequence (HR) is indicated by reduced staining (A_{540}). B–D, apoptosis/necrosis assays. NCI-N87 cells were treated for 1 hour with 10 μmol/L HR or $HM_{85}R$ proteins, and at the indicated times, the cells were analyzed for Annexin-V staining (B); DNA content (C), flow cytometry of cells stained with propidium iodide; and apoptosis/necrosis (D), flow cytometry of cells stained with both PI and Annexin-V. Apoptotic/necrotic cells induced by CP-RUNX3 ($HM_{85}R$) are indicated by accumulation of cells with less than a G_1 DNA content (B), by increased Annexin-V staining (C) and by accumulation of cells staining with both PI and Annexin-V (D).

with less than G_1 DNA content, which occurred primarily at the expense of cells with a G_1 DNA content (Fig. 4C). However, most of the cells with enhanced Annexin-V staining also stained with PI (Fig. 4D), indicative of either late apoptosis or necrotic cell death. The lack of Annexin-V single-positive cells, even at early time points, suggests that the loss of cell viability induced by $HM_{85}R$ results from necrotic cell death. The effect was more pronounced in NCI-N87 cells that had higher basal levels of necrosis than MKN28 cells (data not shown). Unlike the gastric cancer cell lines, CP-RUNX3 did not appear to be toxic to NIH3T3 cells (data not shown).

Antitumor activity of cell-permeable RUNX3

We next assessed the antitumor activity of CP-RUNX3 against human cancer xenografts. NCI-N87 cells were injected subcutaneously into nude mice, tumors were allowed to grow in size to 60 to 80 mm^3, and then the mice were injected subcutaneously near the tumors with 5 mg/kg recombinant RUNX3 proteins (HR, $HM_{57}R$, or $HM_{85}R$) or diluent (PBS) every day for 3 weeks. Mice were observed for an additional 2 weeks after treatments ended (Fig. 5A). $HM_{57}R$ and $HM_{85}R$ significantly suppressed the tumor growth ($P < 0.05$) during the treatment phase. However, once treatment stopped, sustained antitumor activity was observed only in $HM_{85}R$-treated mice (87% inhibition at day 21; 74% at day 35, respectively), whereas the growth of $HM_{57}R$-treated tumors increased, matching the rates observed in control mice. Differences among the tumors from different treatment groups were apparent by external examination (Fig. 5B) and tumors weight (Fig. 5C). While tumor growth was also reduced in mice treated with the HR control protein, which lacks a MTD sequence, the effect was not significant.

CP-RUNX3 was also tested for antitumor activity following systemic rather than local delivery (Fig. 5D). Tumor-bearing mice were prepared as before and were injected intravenously daily for 3 weeks with (i) 15 mg/kg $HM_{85}R$; (ii) 2 control proteins: HR, RUNX3 lacking an MTD sequence, and $HM_{85}E$, which contains EGFP instead of the RUNX3 sequence; or (iii) buffer alone. Although $HM_{85}E$ displayed antitumor activity as compared with the control proteins, the effects were relatively modest (70% inhibition at day 21).

Published OnlineFirst December 10, 2012; DOI: 10.1158/1078-0432.CCR-12-2692

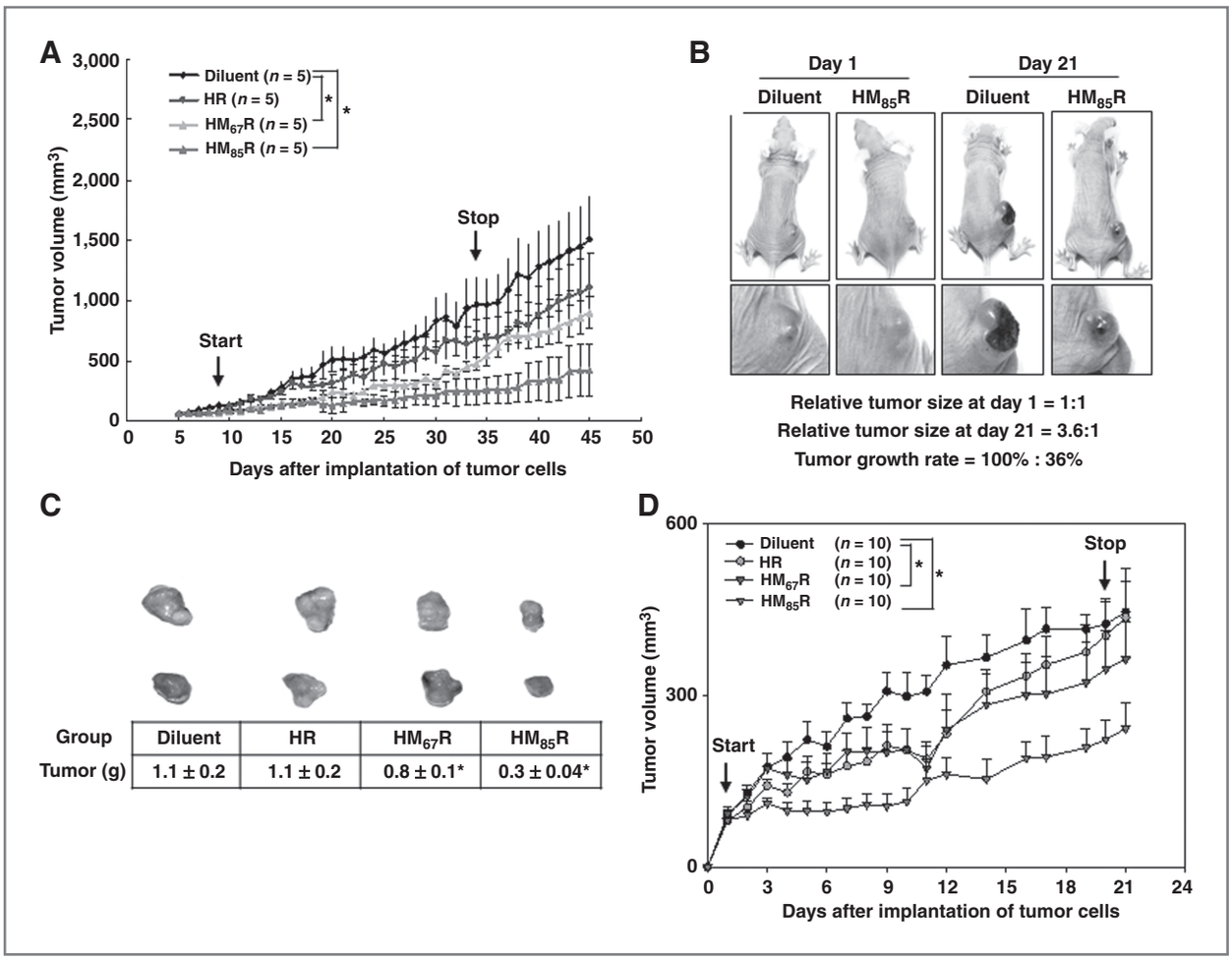

Figure 5. CP-RUNX3 protein suppresses the growth of human gastric tumors in a mouse xenograft model. $HM_{85}R$ significantly suppressed tumor growth (by 87% 21 days after subcutaneous administration) with sustained antitumor activity (74% at day 35). Intravenously administered $HM_{85}R$ was less active than subcutaneously administered protein (70% at day 21). A, suppression of tumors induced by subcutaneous injection of NCI-N87 human gastric cancer cells. After tumors reached a size of 60to 80 mm^3 (start), the mice were injected daily (subcutaneously near the tumor) for 3 weeks with diluent alone (black) or with 100 μg HR (blue), $HM_{57}R$ (green), or $HM_{85}R$ (red). Tumor growth was suppressed to varying degrees after protein therapy ended (stop). *, $P < 0.05$ as determined by Student *t* test. Efficient tumor inhibition, up to 87%, required MTD sequences. B, external appearance of tumor-bearing mice. Representative mice treated with diluent alone or with $HM_{85}R$ were photographed on days 1 and 21 after starting protein therapy. Differences in tumor growth are apparent by external examination. C, representative tumor appearance and weight. Tumors dissected 21 days after treatment with diluent, HR, $HM_{57}R$, and $HM_{85}R$ were photograph and weighed. *, $P < 0.05$ as determined by Student *t* test. D, suppression of tumor growth by intravenous injection of CP-RUNX3. Tumor-bearing nude mice induced by subcutaneous injection of NCI-N87 human gastric cancer cells were treated intravenously for 3 weeks with diluent alone (black) or with 300 μg HR (green), $HM_{85}E$ (blue), or $HM_{85}R$ (red). *, $P < 0.05$ as determined by Student *t* test. Tumor growth was inhibited by 70% (day 21) by CP-RUNX3 ($HM_{85}R$) not by proteins containing a neutral gene (EGFP, $HM_{85}E$) or lacking the MTD sequence (HR).

Antitumor activity of $HM_{85}R$ was accompanied by apoptosis/necrosis as visualized by terminal deoxynucleotidyl transferase–mediated dUTP nick end labeling (TUNEL) and ApopTag staining of tumor sections analyzed 3 weeks after treatment (Fig. 6A) and by changes in biomarker expression linked to RUNX3 signaling, including enhanced levels of $p21^{Waf1}$ (Fig. 6B, top) and lower levels of VEGF (Fig. 6B, bottom), *CCNE* (cyclin E2), *FOS*, and *JUN* (Fig. 6C) at day 21. Loss of $p21^{Waf1}$ expression persisted in $HM_{85}R$-treated tumors at day 35 (Fig. 6D), whereas VEGF levels returned to normal by day 35 (data not shown). In contrast, tumor biomarker expression was not affected in mice treated with the HR control protein, which lacks an MTD sequence. Finally, all of the proteins tested appeared to be well tolerated as assessed by external appearance, activity level, and body weight (Supplementary Fig. S2).

Discussion

The present study investigated the use of MITT to deliver biologically active RUNX3 protein into gastric cancer cells both *in vitro* and *in vivo*. Proteins engineered to enter cells suppressed cell proliferation, wound healing, and survival, consistent with its role as a tumor suppressor. Moreover, the cell-permeable RUNX3 induced changes in biomarker expression, notably $p21^{Waf1}$ and VEGF, consistent with its

Published OnlineFirst December 10, 2012; DOI: 10.1158/1078-0432.CCR-12-2692

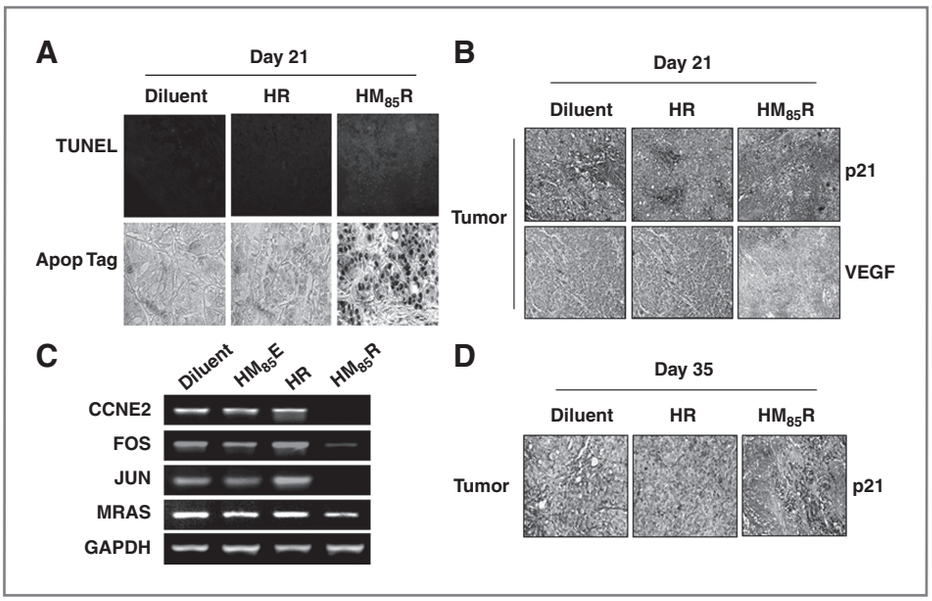

Figure 6. Antitumor activity of CP-RUNX3 proteins. $HM_{85}R$ induced apoptosis/necrosis in tumors accompanied by changes in biomarker expression linked to RUNX3/TGF-β signaling. A, CP-RUNX3 induces tumor cell apoptosis. Sections from paraffin-embedded tumors were prepared after treatment for 3 weeks after protein therapy ended (day 21), and apoptotic cells were visualized by ApopTag and TUNNEL staining. B and D, immunohistochemistry. C, RT-PCR. $HM_{85}R$-induced changes in biomarker expression in tumor xenografts. Tumor sections from mice treated daily for 3 weeks with diluent alone or with 100 μg of either HR or $HM_{85}R$ were sectioned and immunostained with antibodies against $p21^{Waf1}$ or VEGF. Gene expression profile of the tumors obtained from mice treated with HR or $HM_{85}R$ compared to diluent. D, loss of $p21^{Waf1}$ expression persisted in $HM_{85}R$-treated tumors at day 35. GAPDH, glyceraldehyde-3-phosphate dehydrogenase.

known role in TFG-β signaling. The protein also enhanced apoptotic/necrotic cell death of NCI-N87 cells, *in vitro* and apoptosis/necrosis in NCI-N87 tumor xenografts, with changes in $p21^{Waf1}$ and VEGF expression consistent with a direct effect on tumor cells.

The present study used 2 new MTDs, MTD57 and MTD85, to deliver RUNX3 proteins into cultured cells and tumors. These MTD sequences were developed by a process in which predicted leader peptides were first tested for their ability to promote uptake of an EGFP reporter protein by cultured cells, and the sequences were subsequently modified to eliminate charged amino acids, increase the predicted α-helical content, and limit the number of consecutive hydrophobic residues. MTD85 was observed to be a more efficient delivery vehicle than MTD57 as assessed with EGFP and RUNX3 protein cargoes. Consistent with greater protein uptake, MTD85-modified RUNX3 proteins had greater biologic activity both *in vitro* and *in vivo*. Computer models also suggest that MTD85 has a greater α-helical structure than MTD57 (Supplementary Table S1), a feature associated with enhanced protein uptake (29). However, further study will be required to determine protein sequences and/or structures required for optimal protein delivery.

In principle, protein-based therapeutics offers a way to control biochemical processes in living cells under non–steady-state conditions and with fewer off-target effects than conventional small-molecule therapeutics. In practice, systemic protein delivery in animals has proven difficult due to poor tissue penetration and rapid clearance (30, 31). Some success has been achieved using sequences derived from hydrophobic signal peptides to deliver biologically active peptides and proteins to a variety of tissues (including liver, lung, pancreas, and lymphoid tissues). Striking therapeutic benefits have been reported using a small peptide to protect against otherwise lethal inflammatory responses (21, 23–25). Therapeutic benefits have also been achieved using larger cell-permeable proteins including: (i) suppressor of cytokine signaling 3 (SOCS3) to protect animals against lethal inflammation (22), (ii) the NM23 metastasis suppressor to inhibit the seeding and growth of pulmonary metastases (26), and (iii) the cyclin-dependent kinase inhibitor, $p18^{INK4c}$, to inhibit the growth of tumor xenografts (27). As the practical development of cell-permeable proteins has a large empirical component, the present study is part of a larger effort to understand the variables that might predict whether a given protein can be delivered in biologically active form into mammalian cells and tissues. In addition, we wanted to determine whether CP-RUNX3 had activities consistent with tumor suppression and test the feasibility of using RUNX3 as a protein-based therapy to treat gastric cancer, a cancer for which no effective therapies currently exist (35).

The antitumor activity of CP-RUNX3 was comparable with that associated with augmenting *RUNX3* gene expression in tumor cell lines. This is despite the fact that subcutaneous tumors, due to limited vascularization, provide a challenging test of *in vivo* protein delivery and uptake. Thus, the activity of CP-RUNX3 approached the expected theoretical limit as determined by cell-intrinsic RUNX3 biology—consistent with the idea that RUNX3 can function as a

Published OnlineFirst December 10, 2012; DOI: 10.1158/1078-0432.CCR-12-2692

tumor suppressor in gastric cancer. However, this interpretation carries several caveats. First, although mice tolerated high levels of RUNX3 protein without weight loss or obvious adverse effects, the tumor-specific effects of exogenous CP-RUNX3 are potentially nonphysiologic, as protein levels delivered by transduction are higher [compare levels of CP-RUNX3 in cells and tissues, Fig. 2, with levels of endogenous RUNX3 reported elsewhere (refs. 9, 10)]. Moreover the influx of CP-RUNX3 is relatively rapid (within 60 minutes)—a greater rate of change than would be expected in normal cells undergoing cell differentiation or oncogenic transformation. Second, although RUNX3 directly targeted xenografted tumor cells as assessed by changes in $p21^{Waf1}$ and VEGF expression, we cannot exclude the possibility CP-RUNX3 also targets other cells such as vascular endothelium that influence tumor growth and/or survival in the subcutaneous niche.

The antitumor activity of CP-RUNX3 fell short of that achieved by either CP-$p18^{INK4c}$ or CP-MN23, which target cell cycle and metastasis, respectively (26, 27). Moreover, CP-$p18^{INK4c}$ and CP-MN23 produced prolonged therapeutic effects when administered systemically (i.e., by intravenous injection), whereas CP-RUNX3 was most active when administered subcutaneously in regions surrounding the tumors. Therefore, further therapeutic development of CP-RUNX3 will require formulations with improved bioavailability when administered systemically, for example, by using different MTDs or smaller, biologically active RUNX3 domain(s). A full evaluation will require testing CP-RUNX3, both individually and in combination with other agents, and with a variety of cancer models.

Disclosure of Potential Conflicts of Interest

J. Lim is an employee of ProCell Therapeutics, Inc. D. Jo was the founding scientist of ProCell Therapeutics, Inc. and is affiliated to Vanderbilt University at present. Hereby; these two authors disclose a financial interest in the company. No potential conflicts of interest were disclosed by the other authors.

Authors' Contributions

Conception and design: D. Jo
Development of methodology: J. Lim, T. Duong, N. Do, P. Do, D. Jo
Acquisition of data (provided animals, acquired and managed patients, provided facilities, etc.): J. Lim, T. Duong, N. Do, P. Do, D. Jo
Analysis and interpretation of data (e.g., statistical analysis, biostatistics, computational analysis): J. Lim, T. Duong, N. Do, P. Do, J. Kim, H. Kim, W. El-Rifai, H. E. Ruley, D. Jo
Writing, review and/or revision of the manuscripts: H. E. Ruley, D. Jo
Administrative, technical, or material support (i.e., reporting or organizing data, constructing databases): D. Jo
Study supervision: D. Jo

Acknowledgments

The authors thank Dr. Chris Ko for his critical comment and many young scientists who were involved in the early stage of this study for their technical assistance.

Grant Support

This work was supported by grant of the Industrial Strategic Technology Development Program (10032101 to D. Jo) of Ministry of Knowledge Economy, Republic of Korea.

The costs of publication of this article were defrayed in part by the payment of page charges. This article must therefore be hereby marked *advertisement* in accordance with 18 U.S.C. Section 1734 solely to indicate this fact.

Received August 14, 2012; revised November 6, 2012; accepted November 21, 2012; published OnlineFirst December 10, 2012.

References

1. Hartgrink HH, Jansen EP, van Grieken NC, van de Velde CJ. Gastric cancer. Lancet 2009;374:477–90.
2. Yamashita K, Sakuramoto S, Watanabe M. Genomic and epigenetic profiles of gastric cancer: potential diagnostic and therapeutic applications. Surg Today 2011;41:24–38.
3. Li QL, Ito K, Sakakura C, Fukamachi H, Inoue K, Chi XZ, et al. Causal relationship between the loss of RUNX3 expression and gastric cancer. Cell 2002;109:113–24.
4. Chuang LS, Ito Y. RUNX3 is multifunctional in carcinogenesis of multiple solid tumors. Oncogene 2010;29:2605–15.
5. Hanai J, Chen LF, Kanno T, Ohtani-Fujita N, Kim WY, Guo WH, et al. Interaction and functional cooperation of PEBP2/CBF with Smads. Synergistic induction of the immunoglobulin germline Calpha promoter. J Biol Chem 1999;274:31577–82.
6. Chi XZ, Yang JO, Lee KY, Ito K, Sakakura C, Li QL, et al. RUNX3 suppresses gastric epithelial cell growth by inducing p21(WAF1/Cip1) expression in cooperation with transforming growth factor {beta}-activated SMAD. Mol Cell Biol 2005;25:8097–107.
7. Peng Z, Wei D, Wang L, Tang H, Zhang J, Le X, et al. RUNX3 inhibits the expression of vascular endothelial growth factor and reduces the angiogenesis, growth, and metastasis of human gastric cancer. Clin Cancer Res 2006;12:6386–94.
8. Subramaniam MM, Chan JY, Yeoh KG, Quek T, Ito K, Salto-Tellez M. Molecular pathology of RUNX3 in human carcinogenesis. Biochim Biophys Acta 2009;1796:315–31.
9. Ito K, Liu Q, Salto-Tellez M, Yano T, Tada K, Ida H, et al. RUNX3, a novel tumor suppressor, is frequently inactivated in gastric cancer by protein mislocalization. Cancer Res 2005;65:7743–50.
10. Wei D, Gong W, Oh SC, Li Q, Kim WD, Wang L, et al. Loss of RUNX3 expression significantly affects the clinical outcome of gastric cancer patients and its restoration causes drastic suppression of tumor growth and metastasis. Cancer Res 2005;65:4809–16.
11. Wakatsuki K, Yamada Y, Narikiyo M, Ueno M, Takayama T, Tamaki H, et al. Clinicopathological and prognostic significance of mucin phenotype in gastric cancer. J Surg Oncol 2008;98:124–9.
12. Oshimo Y, Oue N, Mitani Y, Nakayama H, Kitadai Y, Yoshida K, et al. Frequent loss of RUNX3 expression by promoter hypermethylation in gastric carcinoma. Pathobiology 2004;71:137–43.
13. Hsu PI, Hsieh HL, Lee J, Lin LF, Chen HC, Lu PJ, et al. Loss of RUNX3 expression correlates with differentiation, nodal metastasis, and poor prognosis of gastric cancer. Ann Surg Oncol 2009;16:1686–94.
14. Brenner O, Levanon D, Negreanu V, Golubkov O, Fainaru O, Woolf E, et al. Loss of Runx3 function in leukocytes is associated with spontaneously developed colitis and gastric mucosal hyperplasia. Proc Natl Acad Sci U S A 2004;101:16016–21.
15. Carvalho R, Milne AN, Polak M, Corver WE, Offerhaus GJ, Weterman MA. Exclusion of RUNX3 as a tumour-suppressor gene in early-onset gastric carcinomas. Oncogene 2005;24:8252–8.
16. Levanon D, Bernstein Y, Negreanu V, Bone KR, Pozner A, Eilam R, et al. Absence of Runx3 expression in normal gastrointestinal epithelium calls into question its tumour suppressor function. EMBO Mol Med 2011;3:593–604.
17. Friedrich MJ, Rad R, Langer R, Voland P, Hoefler H, Schmid RM, et al. Lack of RUNX3 regulation in human gastric cancer. J Pathol 2006;210:141–6.
18. Gorelik L, Flavell RA. Abrogation of TGFbeta signaling in T cells leads to spontaneous T cell differentiation and autoimmune disease. Immunity 2000;12:171–81.
19. Jenkins BJ, Grail D, Nheu T, Najdovska M, Wang B, Waring P, et al. Hyperactivation of Stat3 in gp130 mutant mice promotes gastric

Published OnlineFirst December 10, 2012; DOI: 10.1158/1078-0432.CCR-12-2692

hyperproliferation and desensitizes TGF-beta signaling. Nat Med 2005;11:845–52.
20. Kim BG, Li C, Qiao W, Mamura M, Kasprzak B, Anver M, et al. Smad4 signalling in T cells is required for suppression of gastrointestinal cancer. Nature 2006;441:1015–9.
21. Moore DJ, Zienkiewicz J, Kendall PL, Liu D, Liu X, Veach RA, et al. *In vivo* islet protection by a nuclear import inhibitor in a mouse model of type 1 diabetes. PLoS One 2010;5:e13235.
22. Jo D, Liu D, Yao S, Collins RD, Hawiger J. Intracellular protein therapy with SOCS3 inhibits inflammation and apoptosis. Nat Med 2005;11:892–8.
23. Liu D, Liu XY, Robinson D, Burnett C, Jackson C, Seele L, et al. Suppression of *Staphylococcal Enterotoxin B*-induced toxicity by a nuclear import inhibitor. J Biol Chem 2004;279:19239–46.
24. Liu D, Zienkiewicz J, DiGiandomenico A, Hawiger J. Suppression of acute lung inflammation by intracellular peptide delivery of a nuclear import inhibitor. Mol Ther 2009;17:796–802.
25. Liu XY, Robinson D, Veach RA, Liu D, Timmons S, Collins RD, et al. Peptide-directed suppression of a pro-inflammatory cytokine response. J Biol Chem 2000;275:16774–8.
26. Lim J, Jang G, Kang S, Lee K, Nga DTT, Phuong DTL, et al. Cell permeable NM23 blocks the maintenance and progression of established pulmonary metastasis. Cancer Res 2011;71:7216–25.
27. Lim J, Kim J, Duong T, Lee G, Yoon J, Kim H, et al. Antitumor activity of cell-permeable p18(INK4c) with enhanced membrane and tissue penetration. Mol Ther 2012;20:1540–9.
28. Veach RA, Liu D, Yao S, Chen Y, Liu XY, Downs S, et al. Receptor/transporter-independent targeting of functional peptides across the plasma membrane. J Biol Chem 2004;279:11425–31.
29. Ramamoorthy A, Kandasamy SK, Lee DK, Kidambi S, Larson RG. Structure, topology, and tilt of cell-signaling peptides containing nuclear localization sequences in membrane bilayers determined by solid-state NMR and molecular dynamics simulation studies. Biochemistry 2007;46:965–75.
30. Fischer PM. Cellular uptake mechanisms and potential therapeutic utility of peptidic cell delivery vectors: progress 2001–2006. Med Res Rev 2007;27:755–95.
31. Heitz F, Morris MC, Divita G. Twenty years of cell-penetrating peptides: from molecular mechanisms to therapeutics. Br J Pharmacol 2009;157:195–206.
32. Sung M, Poon GM, Gariepy J. The importance of valency in enhancing the import and cell routing potential of protein transduction domain-containing molecules. Biochim Biophys Acta 2006;1758:355–63.
33. Bangsow C, Rubins N, Glusman G, Bernstein Y, Negreanu V, Goldenberg D, et al. The RUNX3 gene–sequence, structure and regulated expression. Gene 2001;279:221–32.
34. Vichai V, Kirtikara K. Sulforhodamine B colorimetric assay for cytotoxicity screening. Nat Protoc 2006;1:1112–6.
35. Paoletti X, Oba K, Burzykowski T, Michiels S, Ohashi Y, Pignon JP, et al. Benefit of adjuvant chemotherapy for resectable gastric cancer: a meta-analysis. JAMA 2010;303:1729–37.